Doc Ophthalmol (2008) 116:119–127
DOI 10.1007/s10633-007-9105-6

ORIGINAL RESEARCH ARTICLE

Chloroquine retinopathy: lipofuscin- and melanin-related fundus autofluorescence, optical coherence tomography and multifocal electroretinography

Ulrich Kellner · Simone Kellner · Silke Weinitz

Received: 25 September 2007 / Accepted: 5 December 2007 / Published online: 16 December 2007

Abstract *Purpose* To evaluate melanin-related near-infrared fundus autofluorescence (NIA, excitation 787 nm, emission > 800 nm), lipofuscin-related fundus autofluorescence (FAF, excitation 488 nm, emission >500 nm), optical coherence tomography (OCT), and multifocal electroretinography (mfERG) in patients with chloroquine (CQ) retinopathy. *Methods* Two patients with progressed CQ retinopathy underwent clinical examination, ISCEV mfERG evaluation, and FAF and NIA imaging using a confocal scanning laser ophthalmoscope (Heidelberg Retina Angiograph 2) with either a 30° or wide-angle field-of-view. OCT3 imaging was performed in one of these patients. *Results* In the foveola, FAF and NIA were relatively normal. Parafoveal loss of retinal pigment epithelium (RPE) was indicated by absent FAF and NIA. An area of reduced FAF and NIA surrounded the parafoveal region of RPE loss. In the adjacent area, FAF was increased and increased NIA marked the peripheral border of increased FAF. Wide-field imaging revealed increased FAF in association with retinal vessels. Retinal thickness was markedly reduced in the OCT predominantly in the parafoveal region. Visual field loss and mfERG amplitude reduction corresponded to areas with increased or reduced FAF and NIA. *Conclusion* Patterns of FAF and NIA indicate different stages of pathophysiologic processes involving lipofuscin and melanin in the RPE. Combined retinal imaging and functional testing provides further insights in the pathogenesis and development of retinal degenerative disease. An association of CQ retinopathy with retinal vessels architecture is hypothesized.

Keywords Chloroquine retinopathy · Fundus autofluorescence · Multifocal ERG · Near-infrared fundus autofluorescence · Retinal imaging

Abbreviations

CQ	Chloroquine
FAF	Fundus autofluorescence
HCQ	Hydroxychloroquine
NIA	Near-infrared fundus autofluorescence

Chloroquine (CQ) and hydroxychloroquine (HCQ) are frequently used to treat autoimmune disorders. Both may induce an irreversible retinal degeneration, that may develop progressively even after cessation of drug treatment [1, 2]. The detailed pathophysiologic mechanisms of CQ/HCQ retinopathy are still undefined. The disruption of intracellular lysosomal function in retinal pigment epithelial (RPE) cells and retinal neurons is most likely the cause of CQ

U. Kellner (✉) · S. Kellner · S. Weinitz
AugenZentrum Siegburg, Europaplatz 3, 53721 Siegburg, Germany
e-mail: kellneru@retinascience.de

U. Kellner · S. Kellner
RetinaScience, 301212, 53192 Bonn, Germany

retinopathy [3]. The high variability of drug dosage associated with retinopathy and the distribution of retinal abnormalities with prolonged sparing of the fovea indicate modifying factors which are unknown yet [4].

In animal experiments, earliest abnormalities were detected in retinal ganglion cells [5]. However, in both animal experiments and histology of human retinas paracentral photoreceptors showed the most severe damage, whereas other retinal neurons and retinal pigment epithelial (RPE) cells were less severely affected [5–7]. Alteration of the photoreceptor inner and outer segment junction and thinning of the retinal outer nuclear layer was identified with high-resolution optical coherence tomography [8]. Early cone photoreceptor involvement can be revealed with the multifocal electroretinogram (mfERG) [9], which is a sensitive test to detect early stages of CQ/HCQ retinopathy [10–12]. Photoreceptor degeneration is usually accompanied by increased RPE phagocytotic activity and lipofuscin accumulation, and consequently fundus autofluorescence of lipofuscin (FAF) has been reported to identify earliest morphologic changes in CQ/HCQ retinopathy [10]. Due to fluorophores, predominantly A2E, in lipofuscin, FAF allows to detect alterations of lipofuscin distribution in RPE cells and its clinical use has been demonstrated in a multitude of retinal diseases [13, 14].

Recently near-infrared fundus autofluorescence (NIA) has been introduced to measure the autofluorescence of melanin in the RPE and the choroid [15, 16]. Melanin is involved in the degradation of photoreceptor outer segments and serves as a major antioxidant in the RPE cells [17–20].

In the present study, we present previously unreported patterns of RPE alterations detected by FAF, NIA, and OCT imaging in two patients with progressed CQ retinopathy.

Patients and methods

Two female patients with CQ retinopathy examined at the AugenZentrum Siegburg were included in this study. Both patients were not included in our previous study on FAF imaging in CQ retinopathy [10]. The diagnosis was established based on patient and family history, ophthalmoscopy, visual field testing, and full field ERG and mfERG according to the standards of the International Society for Clinical Electrophysiology of Vision as reported previously [10, 21, 22]. Both patients gave informed consent after detailed explanation about the background of the study. The study was performed in adherence to the tenets of the Declaration of Helsinki. The ethics committee decided that approval was not required for this study as commercially available methods were used without modification of the instruments.

In vivo measurement of lipofuscin- and melanin-related autofluorescence was performed after medical dilatation of the pupil (phenylephrine 2.5% and tropicamide 1%, at least 5 mm). Images were obtained with a confocal scanning laser ophthalmoscope (Heidelberg Retina Angiograph 2, Heidelberg Engineering, Heidelberg, Germany) using different camera objectives for either a 30° or a wide-angle field-of-view mode. The image resolution was 768 × 768 pixel. The maximum illumination of a 10 × 10° field-of-view was about 2 mW/cm^2. Focusing was achieved using the near-infrared reflectance mode at 815 nm. FAF imaging was carried out as described in detail previously [10, 23]. Argon laser light (488 nm) was used to excite lipofuscin autofluorescence. A band-pass filter with a cut-off at 500 nm included in the system was inserted in front of the detector. Six pictures per second were recorded and about 10 single images were averaged depending on the fixation of the patient.

NIA imaging was carried out as described by Keilhauer and Delori [16]. Diode laser light (787 nm) was used to excite melanin autofluorescence. A band-pass filter with a cut-off at 800 nm included in the system was inserted in front of the detector. Six pictures per second were recorded and about 15 single images were averaged depending on the fixation of the patient.

Optical coherence tomography was performed with the OCT3 (Carl Zeiss Meditec, Jena, Germany) according to the manufacturers guidelines using fast macular scanning as well as individually placed single scan techniques.

Results

Normal findings

Normal FAF and NIA images show a dark optic disc and dark vessels blocking autofluorescence (Fig. 1).

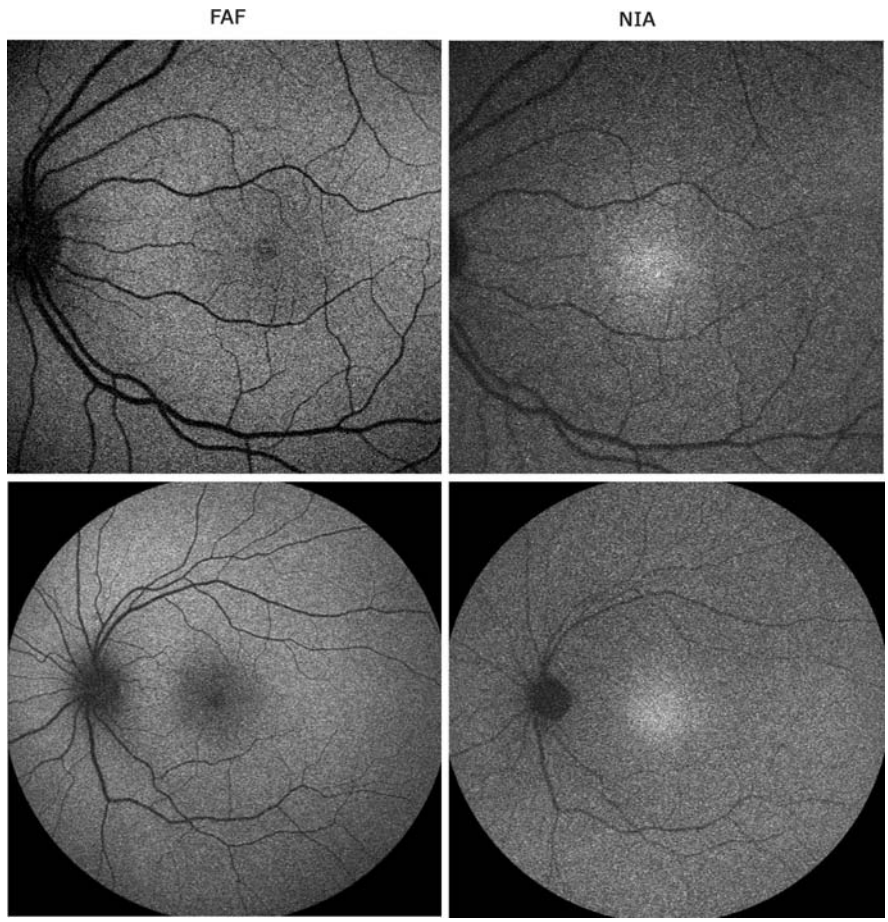

Fig. 1 Representative images of normal FAF and NIA distribution with a 30° field and wide-field imaging in two normal persons

Using a wide-angle field-of-view, FAF and NIA intensity remain unchanged towards the periphery. At the posterior pole, FAF and NIA distribution differ remarkably. The fovea shows reduced FAF to a variable degree due to a blockage by the macular pigment [24, 25]. FAF intensity is highest in the perifoveal region and declines towards the vessel arcades. In contrast, increased NIA is present under the fovea. There is a marked decline of NIA intensity towards the perifoveal region. The intensity and the area of increased NIA are variable. Large choroidal vessels can be visible on normal images.

Patients

Patient #2771, age 51 years, had taken CQ for 20 years (250 mg/d, cumulative dose 1825 g) for the treatment of polyarthritis. She was of normal weight and her general history was normal except polyarthritis. There was no history of other general or ocular disorders and no other medication was taken regularly. In the last two years, problems with night vision were noted. Due to visual acuity loss, cessation of CQ treatment was initiated two months prior to our initial examination. Visual acuity was 20/30 on the right eye and 20/25 on the left eye. On ophthalmoscopy, fine pigment epithelial defects and a slight narrowing of retinal vessels were noted. She was re-examined six and fifteen months later. Her visual acuity remained stable, but she complained about increased difficulties with reading. On ophthalmoscopy progressive parafoveal decreased pigmentation was observed (Fig. 2d).

FAF showed marked alterations at the posterior pole with relative normal foveolar FAF intensity (Fig. 2a–c). Progressive reduction of FAF intensity was noted only in a parafoveal ring (Fig. 2b, c, arrows),

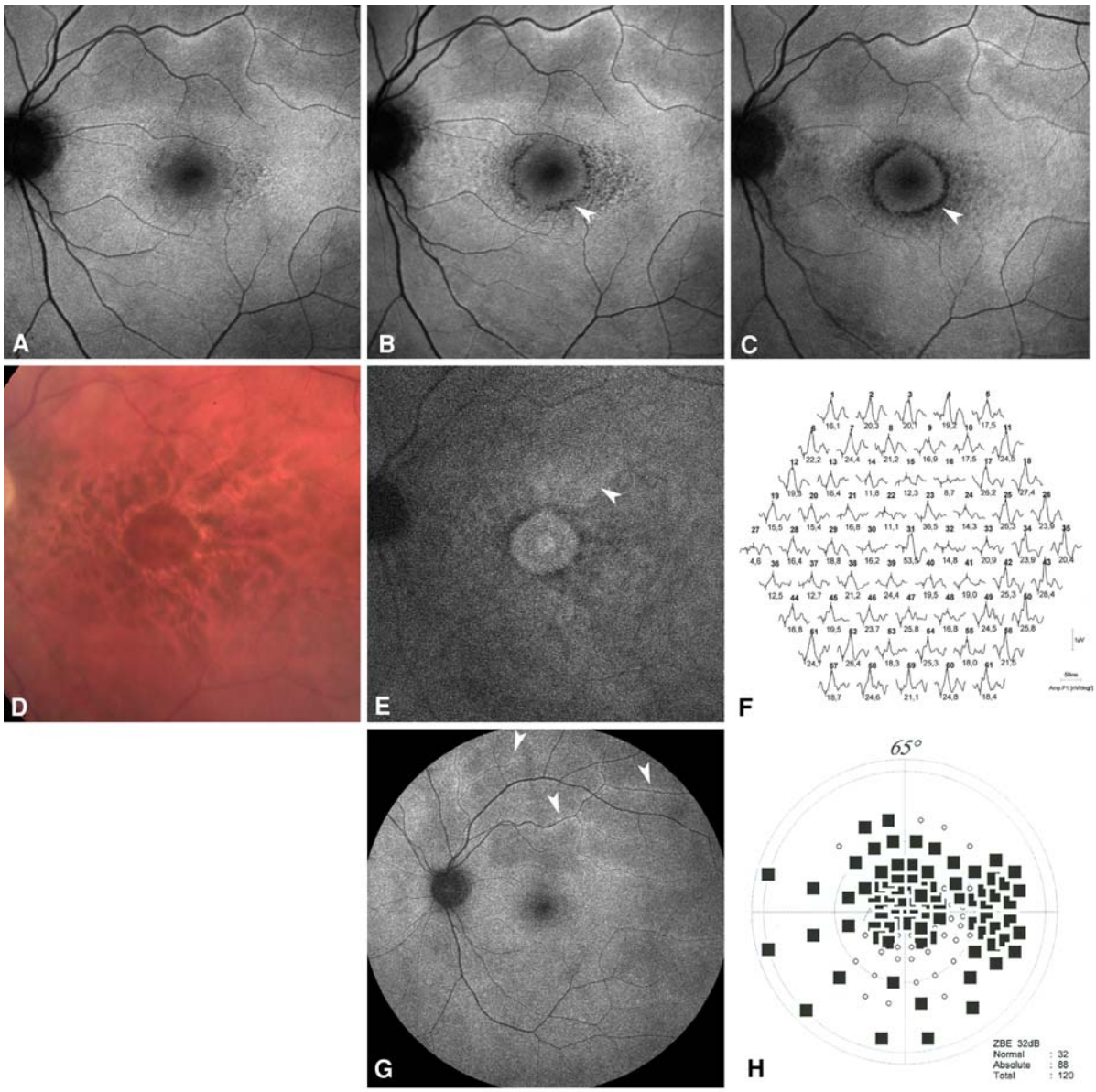

Fig. 2 Chloroquine retinopathy in patient #2771. *Initial visit*: (**a**) Fundus autofluorescence (FAF) of the left eye with normal FAF under the foveola, beginning parafoveal loss of FAF and increased FAF in most areas of the posterior pole and at the vessels of the superior arcade. *Six months later*: (**b**) FAF shows progressed parafoveal loss of FAF (*arrow*). *Fifteen months after the initial visit* (**c**–**h**): (**c**) FAF shows additional progression in the parafoveal ring (*arrow*), but is otherwise similar to the FAF at the initial visit. (**d**) The color image identifies only a pericentral ring of retinal pigment epithelial loss. (**e**) Near-infrared autofluorescence (NIA) with a circumferential loss of NIA surrounding the fovea, preserved NIA under the foveola and slightly increased NIA superior to the fovea (*arrow*). (**f**) MfERG with predominantly pericentral amplitude reduction. (**g**) Wide-field FAF imaging shows increased FAF at the posterior pole and in the nasal and inferior areas; normal FAF is preserved in some superior and temporal areas except alongside the larger arteries (*arrows*). (**h**) Visual field with preserved responses corresponding to the areas of relatively normal FAF

the pericentral and paravascular areas of increased FAF remained unchanged. NIA imaging was available only at the last examination and showed preserved subfoveolar NIA, parafoveal reduced NIA and slightly increased NIA in an area superior to the fovea in which FAF appeared normal (Fig. 2e). The mfERG

corresponded to relatively preserved foveal function and morphology with a moderately reduced central response and with severe reduction in rings 2 and 3 (Fig. 2f). The full-field ERG was performed in the last examination only and showed moderately reduced rod- and cone-related responses indicating a generalized retinal dysfunction. Wide-field FAF imaging documents RPE alterations beyond the vessel arcades towards the periphery and partly corresponding to the retinal vessels (Fig. 2g). Visual field defects corresponded to the areas with increased FAF (Fig. 2h).

Patient #2858 (46 years of age) had taken CQ for 10 years (250 mg/d, cumulative dose 912 g) for treatment of lupus erythematodes. Treatment was stopped 9 months prior to our first examination. She was of normal weight and her general history was unremarkable except lupus erythematodes. There was no history of other general or ocular disorders and no other medication was taken regularly. Visual acuity was 20/40 on both eyes. A paracentral RPE loss was observed on ophthalmoscopy. Ten months later the visual acuity remained unchanged with moderate reading problems. The paracentral RPE loss increased slightly (Fig. 3f).

FAF and NIA were relatively normal in the foveola (Fig. 3a, b). A parafoveal ring of absent FAF and NIA was surrounded by a broader ring of reduced FAF and NIA. The latter was surrounded by an area of increased FAF, which showed increased NIA mostly at the peripheral border. One exception was a small area superior to the fovea with relatively normal FAF and markedly increased NIA. Ten months later, only the parafoveal ring of absent FAF and NIA had progressed (Fig. 3d, e). Wide-field imaging showed additional FAF alterations surrounding the optic disc and extending peripherally alongside the larger retinal vessels (Fig. 3c). Areas of increased and reduced FAF and NIA corresponded to visual field loss and reduced responses in the mfERG (Fig. 3g, h). The full-field ERG was performed only once and showed moderately reduced rod-related responses and mildly reduced cone-related responses indicating a generalized retinal dysfunction. The enlarged blind spot corresponded to the peripapillary area of increased FAF (Fig. 3c, g). OCT scans showed a marked reduction of retinal thickness in all areas of the posterior pole (Fig. 3i). The parafoveal area was most severely reduced.

Discussion

The electroretinographic results in both patients are in accordance with previous reports on full-field ERG [26] and mfERG [26, 27] alterations in progressed CQ retinopathy. Retinal imaging provides additional insights in the pathophysiologic process of CQ retinopathy. New findings in the current study relate to differences between the FAF and NIA images and to the abnormal perivascular distribution of increased FAF. The retinal changes observed with OCT3 have not been previously described in this disorder.

Increased FAF indicates a disease process in the photoreceptor/RPE-complex with increased phagocytotic activity and subsequent lipofuscin accumulation the RPE cells [28]. Reduced or absent FAF corresponds to reduced phagocytotic activity or absence of RPE cells e.g. in geographic atrophy. These FAF alterations have been documented in a multitude of acquired and inherited disorders and are not disease-specific [23, 29–37]. There is consistent evidence that melanin is the major source of NIA, but at present additional contribution of other fluorophores cannot be excluded [15, 16]. Increased NIA corresponds to areas with higher melanin concentration (e.g. nevi) or areas with an ongoing degenerative process [15, 16]. Melanin is involved in phagocytotic processes in the RPE cell and increased NIA could be due to melanogenesis, formation of melanolysosomes, and melanolipofuscin or an alteration of autofluorescence characteristics due to oxidation of melanin [38–41]. Reduced NIA could correspond to a reduction of melanin concentration or activity, whereas absence of NIA corresponds to absence of RPE cells. These NIA alterations have been reported in Stargardt disease [42] (Kellner S; et al, IOVS 2007;48:ARVO E-Abstract 3689), retinitis pigmentosa (Kellner U; et al, IOVS 2007;48:ARVO E-Abstract 3735) and age-related macular degeneration [15, 16] (Kellner U et al, personal communication 2007).

CQ retinopathy is characterized by relative sparing of foveolar function in the presence of parafoveolar dysfunction and subsequent degeneration [1]. Functional correlations are the preservation of a good single letter visual acuity associated with progressive reading difficulties due to the paracentral functional loss as in our patients. The mfERG may show a predominant loss in ring 2 and 3 corresponding to the parafoveal region, although a central reduction as in

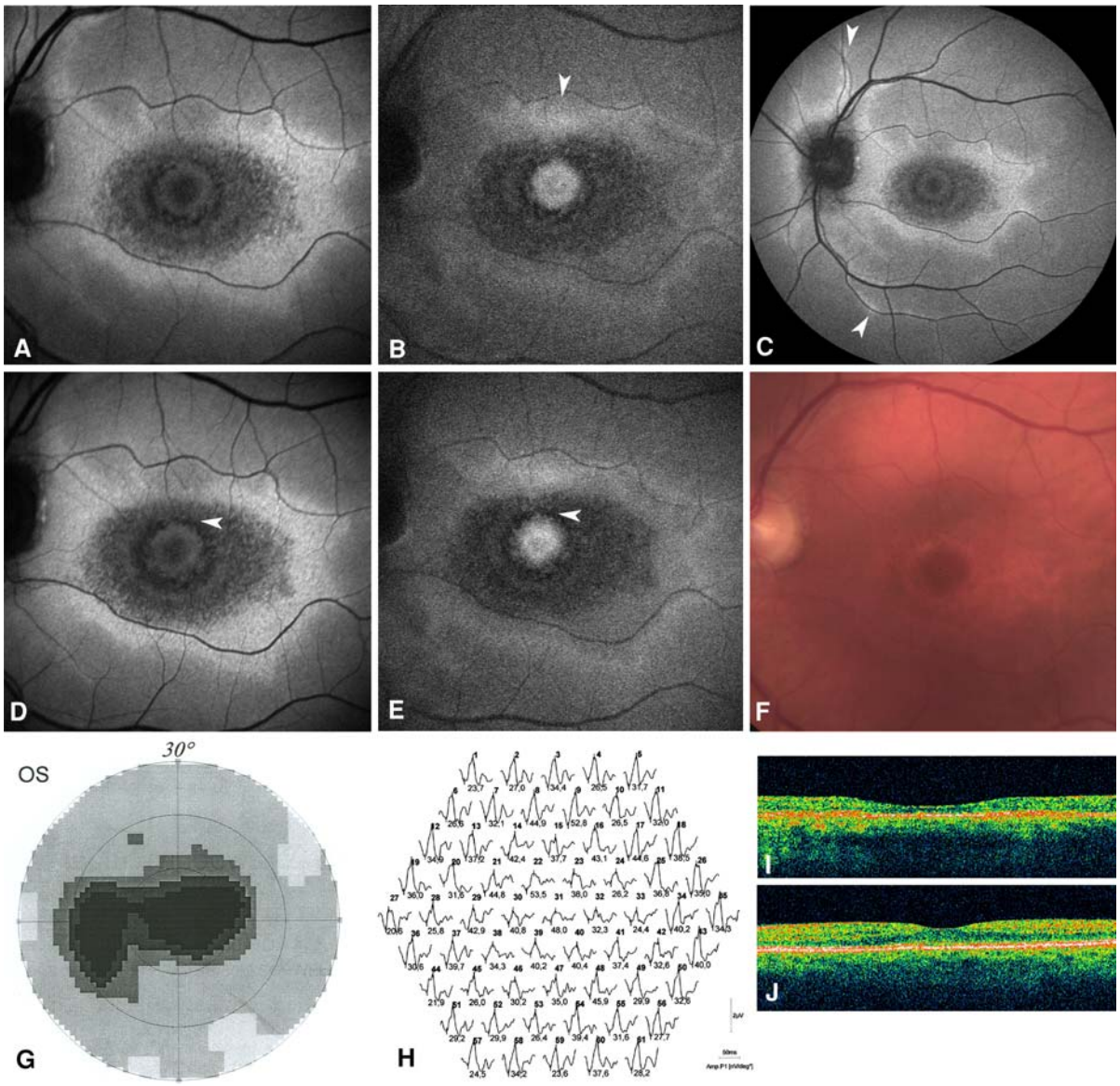

Fig. 3 Chloroquine retinopathy in patient #2858. *Initial visit* (**a**–**c**): (**a**) Fundus autofluorescence (FAF) of the left eye with relatively normal FAF under the foveola, parafoveal loss of FAF and increased FAF towards the perifovea. (**b**) Near-infrared autofluorescence (NIA) with a circumferential loss of NIA surrounding the fovea, preserved NIA under the foveola, increased NIA at the borders of increased FAF and increased NIA superior to the fovea in an area of normal FAF (*arrow*). (**c**) Wide-field FAF imaging shows additional increased FAF surrounding the optic disc and alongside major retinal vessels (*arrows*). *Ten months later* (**d–i**): (**d**) FAF shows additional progression in the parafoveal ring (*arrow*), but is otherwise similar to the FAF at the initial visit. (**e**) NIA is similarly unchanged except for an increased loss in the parafoveal area (*arrow*). (**f**) The color image identifies only a pericentral ring of retinal pigment epithelial loss. (**g**) Visual field loss at the posterior pole and enlarged blind spot. (**h**) MfERG with predominant central amplitude reduction. (**i**) Horizontal OCT scan with reduced retinal thickness especially in the parafoveal area. (**j**) Horizontal OCT scan of a normal person of similar age for comparison

our patients may also develop [10, 27]. The relative preservation of foveolar function corresponds to a relatively normal FAF and NIA distribution in the foveola of our patients. The OCT showed a reduced foveal thickness, but less severe foveal damage compared to the adjacent areas. MfERG reduction

over the parafovea was consistent with the distribution of severely reduced FAF and NIA in both patients. At the border of the fovea RPE damage appeared to be most severe, as the absence of FAF and NIA indicated loss of RPE cells. This is the only region which showed further decline of FAF and NIA intensity during follow-up and explains the increasing reading difficulties of patient no. 2771 despite her preserved single letter acuity. In the adjacent parafoveal area, loss of FAF and NIA intensity were less severe. Beyond the area of RPE cell loss, the FAF intensity increased markedly until it drops again towards the periphery in a presumably less affected area, as can be shown by visual field testing or mfERG. In contrast, NIA is only mildly increased in this area with an additional increase towards the border of increased FAF in one patient. It is of interest that in both patients on both eyes, the increase of NIA was most prominent in an area superior to the fovea, in which FAF was not or only mildly increased. A similar finding has been documented but not discussed in a previously reported patient [15]. The increase of NIA in areas with normal or slightly increased FAF and the increase of NIA at the borders of increased FAF may indicate that increased accumulation of melanin or its derivates corresponds to the initial stage of a degenerative disease process with increasing phagocytotic activity but not increased lipofuscin accumulation. Increased FAF, associated with abnormal lipofuscin accumulation may indicate a more advanced stage of disease with marked RPE cell and presumed photoreceptor damage. Similar differences between FAF and NIA have been observed in Stargardt disease (Kellner S; et al, IOVS 2007;48:ARVO E-Abstract 3689), and age-related macular degeneration (Kellner U et al, personal communication 2007). The final stage with RPE cell death corresponds to melanin and lipofuscin loss indicated by absent NIA and FAF. It is important to note, that the mfERG and visual field show reduced retinal function in areas with reduced as well as increased FAF and NIA.

The correspondence of increased FAF with retinal vessels in the retinal midperiphery is difficult to interpret. Animal experiments have shown that the earliest alterations are observed in retinal ganglion cells, but the most severe damage develops in the photoreceptors [5], which corresponds to the subsequent increase of lipofuscin accumulation as indicated by the increased FAF. No association of retinal vessels and CQ retinopathy has been documented at the posterior pole, although it is likely that the earliest alterations at the posterior pole have been missed due to absent symptoms. The earliest morphologic alteration reported so far was an increased parafoveal ring of FAF when fluorescein angiography and ophthalmoscopy were normal [10]. The most severe damage corresponds to the area of the parafoveal vascular network. One could speculate that longer preservation of the avascular area of the fovea in CQ retinopathy may be due to the lack of retinal vessels. The retinal capillary network is most extensive in the parafovea and around the optic disc, the areas of predominant damage in our patients. It is of interest, that long-term use of CQ corresponds to a reduction of retinal nerve fiber layer thickness [43]. Loss of retinal thickness was also observed in our patient with OCT, although we do not know whether this loss preceded the onset of photoreceptor degeneration. The loss of retinal thickness may alter the distribution of CQ in the retina in association with larger vessels. No obvious retinal vasculopathy was observed in our patients, however, previous episodes of retinal vascular damage cannot be excluded.

Based on the available histological, functional, and morphological findings one could speculate, that the pathogenesis of CQ retinopathy starts with distribution of CQ via the retinal vessels first affecting retinal ganglion cells. Loss of retinal nerve fiber layer thickness could increase CQ levels at the photoreceptor level. Photoreceptors may be more vulnerable compared to ganglion cells and might undergo degeneration predominantly in areas with high intraretinal CQ concentrations. Distribution of CQ from the choroid is unlikely as the fovea overlies the densest choroidal vascular network. Different involvement of retinal vessels in individual general disease could explain part of the variability of the clinical manifestation of CQ retinopathy.

Further studies are needed to understand the pathogenesis of CQ or HCQ retinopathy. The combined application of functional testing and retinal imaging provides means to learn about the pathogenesis of retinal disorders as well as to define optimal settings for patient screening to increase the safety of CQ/HCQ treatment.

References

1. Browning DJ (2002) Hydroxychloroquine and chloroquine retinopathy: screening for drug toxicity. Am J Ophthalmol 133:649–656
2. Shinjo SK, Maia Junior OO, Tizziani VA, Morita C, Kochen JA, Takahashi WY, Laurindo IM (2007) Chloroquine-induced bull's eye maculopathy in rheumatoid arthritis: related to disease duration? Clin Rheumatol 26:1248–1253
3. Mahon GJ, Anderson HR, Gardiner TA, McFarlane S, Archer DB, Stitt AW (2004) Chloroquine causes lysosomal dysfunction in neural retina and RPE: implications for retinopathy. Curr Eye Res 28:277–284
4. Ruther K, Foerster J, Berndt S, Schroeter J (2007) Variabilitat der retinotoxischen Gesamtdosis Chloroquin/Hydroxychloroquin. Ophthalmologe 104:875–879
5. Rosenthal AR, Kolb H, Bergsma D, Huxsoll D, Hopkins JL (1978) Chloroquine retinopathy in the rhesus monkey. Invest Ophthalmol Vis Sci 17:1158–1175
6. Bernstein HN, Ginsberg J (1964) The pathology of chloroquine retinopathy. Arch Ophthalmol 71:238–245
7. Wetterholm DH, Winter FC (1964) Histopathology of chloroquine retinal toxicity. Arch Ophthalmol 71:82–87
8. Rodriguez-Padilla JA, Hedges TR 3rd, Monson B, Srinivasan V, Wojtkowski M, Reichel E, Duker JS, Schuman JS, Fujimoto JG (2007) High-speed ultra-high-resolution optical coherence tomography findings in hydroxychloroquine retinopathy. Arch Ophthalmol 125:775–780
9. Hood DC, Frishman LJ, Saszik S, Viswanathan S (2002) Retinal origins of the primate multifocal ERG: implications for the human response. Invest Ophthalmol Vis Sci 43:1673–1685
10. Kellner U, Renner AB, Tillack H (2006) Fundus autofluorescence and mfERG for early detection of retinal alterations in patients using chloroquine/hydroxychloroquine. Invest Ophthalmol Vis Sci 47:3531–3538
11. Penrose PJ, Tzekov RT, Sutter EE, Fu AD, Allen AW Jr, Fung WE, Oxford KW (2003) Multifocal electroretinography evaluation for early detection of retinal dysfunction in patients taking hydroxychloroquine. Retina 23:503–512
12. Lai TY, Chan WM, Li H, Lai RY, Lam DS (2005) Multifocal electroretinographic changes in patients receiving hydroxychloroquine therapy. Am J Ophthalmol 140:794–807
13. von Ruckmann A, Fitzke FW, Bird AC (1995) Distribution of fundus autofluorescence with a scanning laser ophthalmoscope. Br J Ophthalmol 79:407–412
14. Holz FG, Schmitz-Valckenberg S, Spaide RF, Bird AC (2007) Atlas of fundus autofluorescence imaging. Springer Verlag, Berlin
15. Weinberger AW, Lappas A, Kirschkamp T, Mazinani BA, Huth JK, Mohammadi B, Walter P (2006) Fundus near infrared fluorescence correlates with fundus near infrared reflectance. Invest Ophthalmol Vis Sci 47:3098–3108
16. Keilhauer CN, Delori FC (2006) Near-infrared autofluorescence imaging of the fundus: visualization of ocular melanin. Invest Ophthalmol Vis Sci 47:3556–3564
17. Seagle BL, Rezai KA, Kobori Y, Gasyna EM, Rezaei KA, Norris JR Jr (2005) Melanin photoprotection in the human retinal pigment epithelium and its correlation with light-induced cell apoptosis. Proc Natl Acad Sci USA 102:8978–8983
18. Peters S, Lamah T, Kokkinou D, Bartz-Schmidt KU, Schraermeyer U (2006) Melanin protects choroidal blood vessels against light toxicity. Z Naturforsch [C] 61:427–433
19. Thumann G, Bartz-Schmidt KU, Kociok N, Heimann K, Schraemeyer U (1999) Ultimate fate of rod outer segments in the retinal pigment epithelium. Pigment Cell Res 12:311–315
20. Peters S, Schraermeyer U (2001) Charakteristika und Funktionen des Melanins im retinalen Pigmentepithel. Ophthalmologe 98:1181–1185
21. Marmor MF, Holder GE, Seeliger MW, Yamamoto S (2004) Standard for clinical electroretinography (2004 update). Doc Ophthalmol 108:107–114
22. Marmor MF, Hood DC, Keating D, Kondo M, Seeliger MW, Miyake Y (2003) Guidelines for basic multifocal electroretinography (mfERG). Doc Ophthalmol 106:105–115
23. Renner AB, Tillack H, Kraus H, Kohl S, Wissinger B, Mohr N, Weber BH, Kellner U, Foerster MH (2004) Morphology and functional characteristics in adult vitelliform macular dystrophy. Retina 24:929–939
24. Delori FC, Goger DG, Hammond BR, Snodderly DM, Burns SA (2001) Macular pigment density measured by autofluorescence spectrometry: comparison with reflectometry and heterochromatic flicker photometry. J Opt Soc Am A Opt Image Sci Vis 18:1212–1230
25. Robson AG, Moreland JD, Pauleikhoff D, Morrissey T, Holder GE, Fitzke FW, Bird AC, van Kuijk FJ (2003) Macular pigment density and distribution: comparison of fundus autofluorescence with minimum motion photometry. Vision Res 43:1765–1775
26. Kellner U, Kraus H, Foerster MH (2000) Multifocal ERG in chloroquine retinopathy: regional variance of retinal dysfunction. Graefes Arch Clin Exp Ophthalmol 238:94–97
27. Maturi RK, Yu M, Weleber RG (2004) Multifocal electroretinographic evaluation of long-term hydroxychloroquine users. Arch Ophthalmol 122:973–981
28. Sparrow JR, Boulton M (2005) RPE lipofuscin and its role in retinal pathobiology. Exp Eye Res 80:595–606
29. Delori FC, Staurenghi G, Arend O, Dorey CK, Goger DG, Weiter JJ (1995) In vivo measurement of lipofuscin in Stargardt's disease–Fundus flavimaculatus. Invest Ophthalmol Vis Sci 36:2327–2331
30. von Ruckmann A, Fitzke FW, Bird AC (1997) In vivo fundus autofluorescence in macular dystrophies. Arch Ophthalmol 115:609–615
31. Holder GE, Robson AG, Hogg CR, Kurz-Levin M, Lois N, Bird AC (2003) Pattern ERG: clinical overview, and some observations on associated fundus autofluorescence imaging in inherited maculopathy. Doc Ophthalmol 106:17–23
32. Lois N, Halfyard AS, Bird AC, Holder GE, Fitzke FW (2004) Fundus autofluorescence in Stargardt macular dystrophy-fundus flavimaculatus. Am J Ophthalmol 138:55–63
33. Lorenz B, Wabbels B, Wegscheider E, Hamel CP, Drexler W, Preising MN (2004) Lack of fundus autofluorescence to 488 nanometers from childhood on in patients with early-

onset severe retinal dystrophy associated with mutations in RPE65. Ophthalmology 111:1585–1594
34. Renner AB, Tillack H, Kraus H, Kramer F, Mohr N, Weber BH, Foerster MH, Kellner U (2005) Late onset is common in best macular dystrophy associated with VMD2 gene mutations. Ophthalmology 112:586–592
35. Robson AG, Saihan Z, Jenkins SA, Fitzke FW, Bird AC, Webster AR, Holder GE (2006) Functional characterisation and serial imaging of abnormal fundus autofluorescence in patients with retinitis pigmentosa and normal visual acuity. Br J Ophthalmol 90:472–479
36. Renner AB, Kellner U, Cropp E, Preising MN, MacDonald IM, van den Hurk JA, Cremers FP, Foerster MH (2006) Choroideremia: variability of clinical and electrophysiological characteristics and first report of a negative electroretinogram. Ophthalmology 113:2066 e2061–2010
37. Bindewald A, Bird AC, Dandekar SS, Dolar-Szczasny J, Dreyhaupt J, Fitzke FW, Einbock W, Holz FG, Jorzik JJ, Keilhauer C, Lois N, Mlynski J, Pauleikhoff D, Staurenghi G, Wolf S (2005) Classification of fundus autofluorescence patterns in early age-related macular disease. Invest Ophthalmol Vis Sci 46:3309–3314
38. Smith-Thomas L, Richardson P, Thody AJ, Graham A, Palmer I, Flemming L, Parsons MA, Rennie IG, MacNeil S (1996) Human ocular melanocytes and retinal pigment epithelial cells differ in their melanogenic properties in vivo and in vitro. Curr Eye Res 15:1079–1091
39. Peters S, Kayatz P, Heimann K, Schraermeyer U (2000) Subretinal injection of rod outer segments leads to an increase in the number of early-stage melanosomes in retinal pigment epithelial cells. Ophthalmic Res 32:52–56
40. Feeney-Burns L, Hilderbrand ES, Eldridge S (1984) Aging human RPE: morphometric analysis of macular, equatorial, and peripheral cells. Invest Ophthalmol Vis Sci 25: 195–200
41. Buchanan TA, Gardiner TA, Archer DB (1984) An ultrastructural study of retinal photoreceptor degeneration associated with bronchial carcinoma. Am J Ophthalmol 97:277–287
42. Cideciyan AV, Swider M, Aleman TS, Roman MI, Sumaroka A, Schwartz SB, Stone EM, Jacobson SG (2007) Reduced-illuminance autofluorescence imaging in ABCA4–associated retinal degenerations. J Opt Soc Am A Opt Image Sci Vis 24:1457–1467
43. Bonanomi MT, Dantas NC, Medeiros FA (2006) Retinal nerve fibre layer thickness measurements in patients using chloroquine. Clin Experiment Ophthalmol 34:130–136